Time-division multiplexing-based BOTDA over 100 km sensing length

Yongkang Dong,[1,2] Liang Chen,[1,*] and Xiaoyi Bao[1,3]

[1]Fiber Optics Group, Department of Physics, University of Ottawa, Ottawa, Ontario, K1N 6N5, Canada

[2]e-mail: aldendong@gmail.com

[3]e-mail: Xiaoyi.Bao@uottawa.ca

*Corresponding author: Liang.Chen@uottawa.ca

We propose and demonstrate a high-performance and long-range Brillouin optical time-domain analysis (BOTDA) based on time-division multiplexing measurement, where a probe pulse and a pump pulse are used to perform the measurement on a selected sensing section, and the measurement of the entire sensing fiber is realized by combining the series measurements over different sections through changing the delay time between the two pulses. In experiment, a 100 km sensing fiber is divided into 11 sections based on the gain-controlled principle, and spatial resolutions of 0.6 m and 2 m are obtained at the end of 75 km and 100 km, respectively. © 2011 Optical Society of America

OCIS codes: 190.4370, 060.2370, 290.5900.

Brillouin scattering in fibers has been shown the ability to sense the temperature and strain variations, and based on this finding, the distributed sensors including spontaneous scattering-based Brillouin optical time-domain reflectometry (BOTDR) [1,2] and stimulated scattering based Brillouin optical time-domain analysis (BOTDA) [3–6] have been developed. For BOTDR, the two-way fiber loss of 0.4 dB/km leads to a significant reduction in Brillouin signal as the sensing range is extended, for example, 20 dB for 50 km, and 40 dB for 100 km. In a BOTDA, both the probe and pump waves experience only one-way fiber loss, and stimulated Brillouin scattering (SBS) intensifies the Brillouin signal, thus improving the signal-to-noise ratio (SNR). However, in a BOTDA system, the pump-pulse depletion in Brillouin gain-based sensor or probe-pulse excess amplification in Brillouin loss-based sensor can result in a spectrum distortion, and consequently, in systematic measurement error at the far end of the sensing fiber, which is the main limitation to further extend the sensing range beyond 50 km [7,8]. More recently, in-line Raman amplifiers were used to extend the sensing length to 75 km with a spatial resolution of 2 m [9] and 10 m [10], respectively, where pump depletion could be avoided, because only a low-level probe wave was needed with the fiber loss compensated by the Raman gain.

Usually, a conventional BOTDA includes a probe pulse and a cw pump in a Brillouin loss-based sensor. Because of the fiber attenuation, for a long sensing fiber without in-line amplifiers, the probe and pump powers should be increased to obtain adequate SNR. However, for the worst case with a uniform Brillouin frequency shift (BFS), the probe pulse can interact with the cw pump throughout the entire sensing fiber, which may cause the probe pulse excess amplification and Brillouin spectrum distortion, and thus limit the sensing range [8]. In this Letter, we propose a high-performance long-range BOTDA based on time-division multiplexing measurement, where the sensing range can be extended by multiple measurements along the sensing fiber through the delay-controlled pump pulse. The simple structure of the system is maintained without using an in-line optical amplifier. We demonstrate this technique over a 100 km sensing fiber, obtaining a spatial resolution of 0.6 m and 2 m at the end of 75 km and 100 km, respectively.

Previously, a similar time-division pump-probe scheme was used in a Brillouin optical correlation domain analysis (BOCDA) to select the correlation peak and thus extend its sensing range to 250 m [11]. In our scheme, instead of a pulse and a cw wave as used in a conventional BOTDA, two pulses, i.e., a probe pulse and a pump pulse are used to perform the measurement. The spatial resolution is still defined by the probe-pulse width, while the sensing length is determined by the pump-pulse width. The delay between the probe pulse and the pump pulse can be changed to select the sensing section where the probe pulse interacts with the pump pulse. The measurement of the entire sensing fiber is realized by implementing the measurement for each sensing section through changing the delay between the two pulses, which is named as time-division multiplexing measurement in this letter. Because the interaction length is determined by only the pump-pulse width instead of the entire fiber, the pump power can be increased to enhance the Brillouin interaction in individual sections to improve the SNR without the excess amplification on the probe pulse.

The division of the 100 km sensing fiber according to the gain-controlled principle is shown in Table 1, where the Brillouin gain parameter is controlled at a low level to avoid excess amplification on the probe pulse in each section [8]. The entire sensing fiber is divided into 11 sections with different lengths, where the sequence number of the section is assigned in terms of the propagation direction of the probe pulse, i.e., the probe pulse goes through the sensing fiber from the first section to the eleventh section. The effective interaction length of the nth section is given by $L_{eff}^n = [1 - \exp(-\alpha L_n)]/\alpha$, where α is the fiber attenuation coefficient and L_n is the fiber length of the nth section. Disregarding the pump depletion in individual sections, the Brillouin gain parameter in the nth section is given by $G_n = g_B P_n L_{eff}^n / A_{eff}$, where g_B is

Table 1. Division of 100 km Sensing Fiber

Number of Section	Length (km)	Brillouin Gain	Pump Pulse Width (μs)
1	50	0.34	500
2	14	0.33	140
3	9	0.35	90
4	6	0.33	60
5	5	0.36	50
6	4	0.35	40
7	3	0.31	30
8	3	0.35	30
9	2	0.27	20
10	2	0.29	20
11	2	0.32	20

the Brillouin gain coefficient, A_{eff} is the effective core area, and P_n is the pump pulse power when it arrives at the initial point of the nth section. The normalized Brillouin gain coefficient g_B/A_{eff} of the MetroCor fiber used in the experiment is measured to be 0.1669 W^{-1} m^{-1}. Considering the 1 mW pump-pulse power used in the experiment, the calculated Brillouin gain parameter in individual sections ranges from 0.27 to 0.36 as shown in Table 1, where the low-level Brillouin gain parameters ensure no excess amplification and thus nondistorted spectrum in each section. Because the pump pulse goes from the eleventh section to the first section, the pump-pulse power attenuation allows a longer section length while still keeping a low-level gain; for example, with a Brillouin gain parameter of 0.32 in the eleventh section, the sensing length is only 2 km, while with a Brillouin gain parameter of 0.34 in the first section, the sensing length can be up to 50 km.

Different pump pulse widths are used, corresponding to the fiber length in individual sections, as shown in Table 1, and the delay between the two pulses is controlled to make sure they interact with each other at the selected section, for example, a 500 μs pump pulse is used in the measurement of the first section with 50 km length, where the probe pulse meets the front edge of the pump pulse at the initial point of the section and meets the rear edge of the pump pulse at the end point of the section.
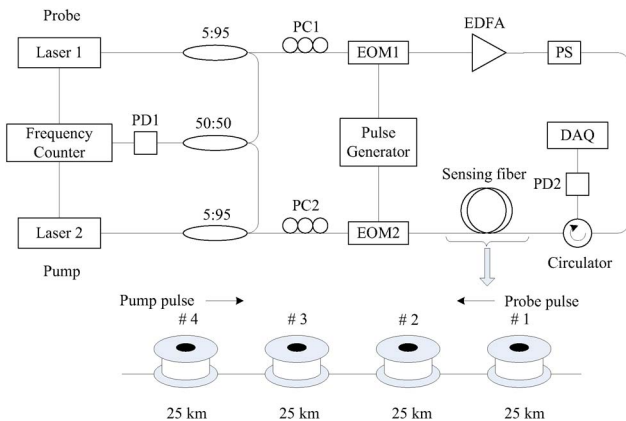

Fig. 1. (Color online) Experimental setup. PD, photodetector; PC, polarization controller; PS, polarization scrambler; EOM, electro-optic modulator; EDFA, erbium-doped fiber amplifier; C, circulator; DAQ, data acquisition.

The experimental setup is shown in Fig. 1. Two narrow-linewidth fiber lasers operating at 1550 nm are used to provide the probe and pump waves whose frequency difference is locked by a microwave frequency counter. A pulse generator is used to drive two high extinction-ratio (>45 dB) electro-optic modulators to generate the probe pulse and the pump pulse, where their delay can be precisely controlled. Before launched into the sensing fiber, the probe pulse is amplified by an erbium-doped fiber amplifier (EDFA). A polarization scrambler is used to change the polarization state of the probe pulse continuously to reduce the polarization-mismatching-induced fluctuation on the signal by averaging a large number of signals, where 2000 times averaging is used in our experiment.

MetroCor fiber with normal dispersion is used as the sensing fiber to avoid the modulation instability (MI) effect induced by the high power probe pulse [8,12], and four spools of 25 km fiber are used to achieve 100 km sensing range, where the sequence number of the spool is also assigned in terms of the propagation direction of the probe pulse, as shown in Fig. 1. Although they are the same type fiber, their BFSs are slightly different; at the room temperature, the BFS of the first and second spool fibers is 10,535 MHz, the third spool fiber is 10,580 MHz, and the fourth spool fiber is 10,530 MHz.

A high-power probe pulse can be used to intensify the Brillouin interaction without the MI effect using normal dispersion fiber; however, the further increase in power will be limited by the stimulated Raman scattering (SRS) [12], where the SRS can also deplete the probe pulse and thus decrease the Brillouin signal significantly as would the MI effect. To avoid the SRS, the maximum probe pulse power used in the following experiments is 1 W, which is below the threshold of the SRS in the 100 km sensing fiber. The time traces of Brillouin signal for all of the sections are shown in Fig. 2, where the probe pulse width is 50 ns and the pump pulse power is 1 mW. The frequency offset between the probe and pump waves is locked at 10,535 MHz for the first section and is 10,580
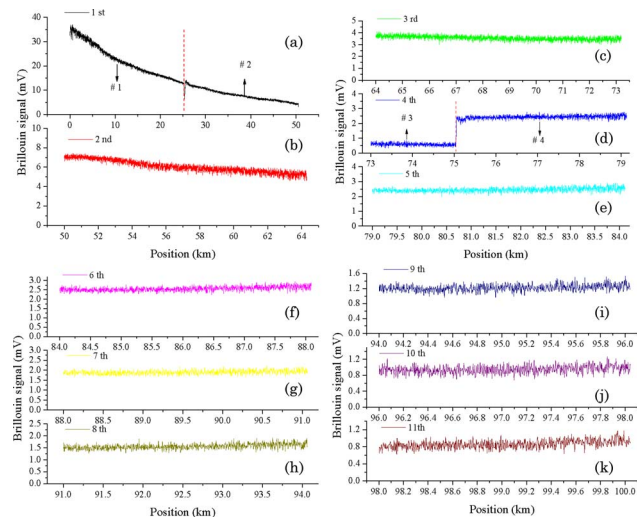

Fig. 2. (Color online) Time traces of the Brillouin signal for 11 sections. The frequency offset between the probe and pump waves is locked at 10,535 MHz for (a), 10,580 MHz for (b) and (c), and 10,530 MHz for (d)–(k).
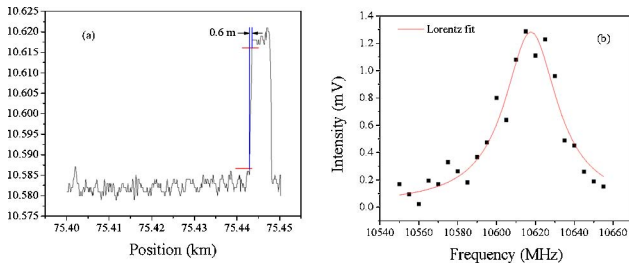
Fig. 3.   (Color online) (a) Measured BFS as a function of the position and (b) a typical spectrum of the heated fiber near the end of 75 km with a fitted linewidth of 32 MHz.
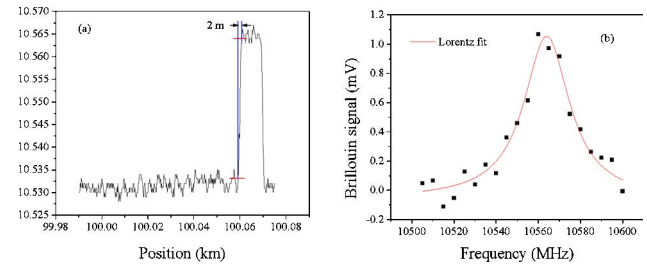

Fig. 4.   (Color online) (a) Measured BFS as a function of the position and (b) a typical spectrum of the heated fiber near the end of 100 km with a fitted linewidth of 26 MHz.

MHz for the second and third sections; for the rest of the sections, it is fixed at 10,530 MHz. The high-power probe pulse can introduce considerable Rayleigh scattering noise in the Brillouin signal, so for the measurement of the first section we use only the 200 mW probe pulse, which can provide sufficient signal while significantly reducing the Rayleigh noise. The Brillouin signal of the first section is shown in Fig. 2(a), where the signal from the first spool fiber is to the left of the dashed line and the signal from the second spool fiber is to the right of the dashed line.

For measurement of the remaining sections, the probe pulse power is increased to 1 W, while the Rayleigh noise is much reduced owing to the attenuated probe pulse power. The second, third, and, to the left of the dashed line in the fourth, sections belong to the third spool fiber, as shown in Fig. 2(b)–2(d). To the right of the dashed line in the fourth section, and the remaining sections, belong to the fourth spool fiber, as shown in Figs. 2(d)–2(k). The 50 ns probe pulse defines a 5 m spatial resolution throughout the entire 100 km sensing fiber.

A higher spatial resolution can be obtained by using differential pulse pair [13,14]. A 2 mW and 30 μs pump pulse was used to measure the last 3 km of the third spool fiber, from 72.5 km to 75.5 km, where a 5 m fiber was heated to 65 °C near the end of the third spool fiber. A 50/55 ns pulse pair was used to obtain the differential signal, and the results are shown in Fig. 3. Figure 3(a) gives the fitted BFS from the measured spectrum as a function of the position, where the rise edge of the transition region indicates a spatial resolution of 0.6 m, and the standard deviation of the BFS is $\sim \pm 2$ MHz, corresponding to a temperature accuracy of ± 2 °C; Fig. 3(b) shows a typical measured spectrum of the heated fiber with a fitted linewidth of 32 MHz.

We also made a measurement near the end of the 100 km fiber by heating a 10 m fiber to 65 °C at the end of the fourth spool fiber. A 10 μs pump pulse was used to measure the last 1 km of the fourth spool fiber, and the results are shown in Fig. 4. A spatial resolution of 2 m is obtained from a 100/120 ns pulse pair, which can be seen from Fig. 4(a). Figure 4(b) shows a typical measured spectrum of the heated fiber with a fitted linewidth of 26 MHz, and the standard deviation of the BFS is

$\sim \pm 2$ MHz, corresponding to a temperature accuracy of ± 2 °C.

To summarize, we have proposed and demonstrated a high-performance and long-range time-division multiplexing-based BOTDA. To avoid excess amplification and enhance the Brillouin interaction, the entire sensing fiber is divided into multiple sections, and the sensing range is extended by the combination of measurements in different sections. The trade-off is that the multiple measurements require additional time. Because fiber attenuation is the only limitation factor, rather than the nonlinear effects, the sensing range is believed to be further extended through the compensation of the fiber loss.

References
1. S. M. Maughan, H. H. Kee, and T. P. Newson, Opt. Lett. **26**, 331 (2001).
2. M. N. Alahbabi, Y. T. Cho, and T. P. Newson, J. Opt. Soc. Am. B **22**, 1321 (2005).
3. S. Diaz, S. F. Mafang, M. Lopez-Amo, and L. Thevenaz, IEEE Sens. J. **8**, 1268 (2008).
4. Y. Dong, X. Bao, and W. Li, Appl. Opt. **48**, 4297 (2009).
5. M. A. Soto, G. Bolognini, F. D. Pasquale, and L. Thevenaz, Opt. Lett. **35**, 259 (2010).
6. H. Liang, W. Li, N. Linze, L. Chen, and X. Bao, Opt. Lett. **35**, 1503 (2010).
7. T. Horiguchi, K. Shimizu, T. Kurashima, M. Tateda, and Y. Koyamada, J. Lightwave Technol. **13**, 1296 (1995).
8. Y. Dong, L. Chen, and X. Bao, Appl. Opt. **49**, 5020 (2010).
9. F. R. Barrios, S. M. Lopez, A. C. Sanz, P. Corredera, J. D. A. Castanon, L. Thevenaz, and M. G. Herraez, J. Lightwave Technol. **28**, 2162 (2010).
10. X. H. Jia, Y. J. Rao, L. Chen, C. Zhang, and Z. L. Ran, J. Lightwave Technol. **28**, 1624 (2010).
11. K. Hotate and H. Arai, Proc. SPIE **5855**, 184 (2005).
12. M. N. Alahbabi, Y. T. Cho, T. P. Newson, P. C. Wait, and A. H. Hartog, J. Opt. Soc. Am. B **21**, 1156 (2004).
13. L. Thevenaz and S. F. Mafang, Proc. SPIE **7004**, 70043N (2008).
14. W. Li, X. Bao, Y. Li, and L. Chen, Opt. Express **16**, 21616 (2008).